



PERGAMON

Atmospheric Environment 34 (2000) 2399–2412

ATMOSPHERIC
ENVIRONMENT

www.elsevier.com/locate/atmosenv

Impingement of rain drops on a tall building

V. Etyemezian^{a,*}, C.I. Davidson^a, M. Zufall^{a,1}, W. Dai^{a,2}, S. Finger^a, M. Striegel^b

^aDepartment of Civil and Environmental Engineering, Carnegie Mellon University, Pittsburgh, PA 15213, USA

^bNational Center for Preservation Technology and Training, NSU Box 5682, Natchitoches, LA 71497, USA

Received 10 August 1998; received in revised form 22 September 1999; accepted 22 September 1999

Abstract

Soiling on the walls of limestone buildings can be washed off when the surface erodes due to rain impingement. In this study, the delivery of rain to the 42-story Cathedral of Learning in Pittsburgh, Pennsylvania, represented by a 30 m × 30 m × 160 m rectangular block, was modeled using the RNG $K-\epsilon$ model for turbulence and Lagrangian trajectory calculations for individual rain drops. Local Effect Factors (LEF) for the rectangular block compared well with earlier work in the literature. LEFs increased with wind speed, raindrop size, and height along the block. Wind speed, direction, and rain intensity were measured continuously over a seven-week period and provided input parameters for modeling rain fluxes to the Cathedral of Learning. Model results suggested that sections of the building receiving larger amounts of rain corresponded to white areas, indicating that rain fluxes have a significant effect on the soiling patterns. Intermediate wind speeds (2.5 and 5 m s⁻¹) resulted in high rain fluxes. Although less frequent, high wind speeds also resulted in high rain fluxes. Much of the rain was delivered to the block as 1.25 and 2.5 mm drops with 5 mm drops having a smaller effect. Consideration of wind incidence angles other than 0° was shown to be important for future modeling efforts. © 2000 Elsevier Science Ltd. All rights reserved.

Keywords: Soiling; Buildings; Driving rain; Acid rain; CFD

1. Introduction

Rain has been shown to be an important agent in determining the extent of calcareous stone erosion and the patterns of surface soiling on buildings (Amoroso and Fassina, 1983; Sherwood et al., 1990). For example, in polluted areas, delivery of acidic rain to the surface of a building can accelerate erosion. Even clean rain is believed to be responsible for some erosion of the surface (Livingston, 1992). Particles that deposited on the surface may be removed as a consequence of rain washing. Thus, areas of a building that are exposed to driving rain are less likely to be soiled than those areas that are protected.

In this study, the flux of rain is estimated for several areas of the walls of the Cathedral of Learning (Fig. 1) on the University of Pittsburgh campus. The building is 42 stories high and is made of Indiana limestone. Built during 1926–1937, the walls are heavily soiled in some areas. This is attributed to pollutant emissions from mobile and stationary sources in the vicinity. The results of the modeling effort are presented in two parts. First, we examine the effect of meteorological conditions and raindrop sizes on the delivery of rain to the outside walls of a building shaped like a tall rectangular block. This is accomplished by computing the rain flux for several hypothetical values of wind speed, wind direction, and raindrop size. Second, we use meteorological data obtained near the Cathedral to estimate the total amount of rain that is delivered to the walls of the Cathedral. The spatial distribution of rain fluxes is compared with observed soiling patterns at the Cathedral.

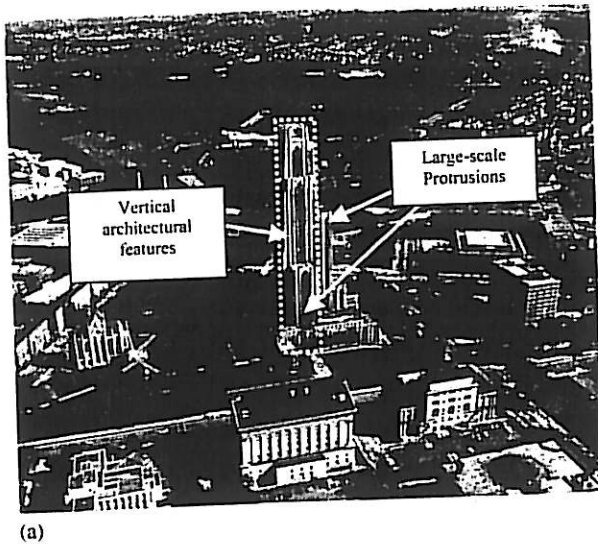
Other work at the Cathedral of Learning has focused on changes in soiling patterns observed in archival

*Corresponding author. Present address: Desert Research Institute, 755 E. Flamingo Rd., Las Vegas, NV 89119, USA.

E-mail address: vic@dri.edu (V. Etyemezian).

¹Current address: NERL, EPA, RTP, NC, USA.

²Current address: Trinity Consultants, 12801 N. Central Expressway, Suite 1200, Dallas, TX, USA.



(a)

| | | |
|-----|----|-----|
| LS5 | C5 | RS5 |
| LS4 | C4 | RS4 |
| LS3 | C3 | RS3 |
| LS2 | C2 | RS2 |
| LS1 | C1 | RS1 |

(b)

Fig. 1. (a) Photograph showing Fifth Avenue side of Cathedral of Learning © 1984, Janosky Studios, Pittsburgh, Pennsylvania. Dashed outline is the part of the Cathedral that is represented by the rectangular block, and (b) Division of block face into 15 equal sections.

photographs, and consideration of changes in air pollutant concentrations and dustfall since the Cathedral was constructed (Tang et al., 1999; Davidson et al., 1999). Etyemezian et al. (1998) measured airborne concentrations and deposition of various aerosol and gaseous chemical species near the walls of the Cathedral. It was determined that neither concentrations nor deposition varied greatly over the height of the building; the lack of gradients was attributed to a well-mixed atmosphere impinging on the Cathedral from upwind and possibly rapid vertical mixing in the immediate vicinity of the building. Soiling patterns on the building were

hypothesized to be the result of variability in rain impingement on the walls. Testing this hypothesis is a focus of the current paper.

2. Methods

Modeling of rain impingement on the walls of the Cathedral of Learning was accomplished in several steps. First, the air flow field around a rectangular block with the same approximate dimensions as the Cathedral was computed numerically. Second, trajectories of individual rain drops, released above the block and subjected to the computed flow field, were calculated; the fate of each drop, i.e. whether it impacted on a surface of the block or the ground, was recorded. These two steps are partly based on earlier work by Choi (1993), allowing for comparison of results of this paper with his earlier work. Third, measurements of rain intensity, wind speed, and wind direction were obtained for a period of seven weeks at a location near the Cathedral. Combined with the results from the first two steps, this last step allowed for estimation of rain delivery to the four sides of the rectangular block used to represent the Cathedral of Learning.

2.1. Air flow

The shape of the Cathedral of Learning was approximated by a $30 \text{ m} \times 30 \text{ m} \times 160 \text{ m}$ rectangular block ($L \times W \times H$) for most model runs. This approximation helped reduce computational effort in two ways, namely by decreasing the detail of the geometry and also by rendering the flow field symmetrical about the plane that bisects the block along the primary direction of flow. The effect of nearby buildings was not considered since the Cathedral is much taller than any of the surrounding buildings. The reader is referred to Karagiozis et al. (1997) for an examination of the flow field and raindrop trajectories around buildings that exert an influence on one another.

The air flow field was modeled in three dimensions using FLUENT, a commercially available computational fluid dynamics software package (FLUENT Inc, Lebanon, NH). The Reynolds-averaged Navier-Stokes and continuity equations were solved numerically to obtain the steady-state velocity field. Closure was achieved with the aid of the Re-Normalization Group $K-\epsilon$ (RNG) equations, where K is the turbulent kinetic energy and ϵ is the turbulent kinetic energy dissipation. Application of Re-Normalization Group Theory to turbulence phenomena has been discussed elsewhere (Sulem et al., 1979; Giles, 1994). While largely similar to the standard $K-\epsilon$ model (Launder and Spalding, 1974; Rodi, 1980), the RNG model contains slightly different constants in the transport equations for K and ϵ and an additional source term in the transport equation for ϵ .

The accuracy of the RNG $K-\epsilon$ model was assessed by simulating the flow around a cube ($L = W = H$) immersed in a boundary layer. This calculation was performed at wind incidence angles of 0 and 45°. A considerable body of information on these flow configurations, both from wind tunnel experiments (Castro and Robins, 1977; Ogawa et al., 1983; Minson et al., 1995) and from other CFD efforts (Patterson and Apelt, 1989; Zhou and Stathopoulos, 1996; Murakami et al., 1996; Selvam, 1996), was available from the literature. In general, the major features of the flow were captured well by the RNG model. These included separation of the boundary layer at the ground near the upstream face, separation at the windward edges of the cube, development of a horizontal horseshoe vortex at ground level near the windward face, and the formation of vertical vortices on the leeward faces of the cube (Hosker, 1984).

The flow field around the rectangular block ("block" hereafter) was also computed at wind incidence angles of 0 and 45°. Since the air flow around the block is symmetric at these angles, it was possible to implement the CFD model for only half the physical domain of the flow field. For the 0° case, the computational domain extended 600 m in the upwind direction, 670 m downwind of the block, 150 m from the plane of symmetry, and 540 m from the ground. The structured mesh, containing 1.8×10^5 nodes, was constructed so that the density of nodes was highest near the block and ground. For flow at 45° to the block, the physical size of the computational domain was reduced because the block is more streamlined in this configuration. The domain extended 480 m upwind, 560 m downwind, 120 m from the plane of symmetry, and 480 m from the ground. Despite the reduction in the physical size of the domain, it was necessary to use more nodes in the 45° case (2.7×10^5) in order for the numerical solution to converge.

At the top boundary, the side boundary, and the plane of symmetry, components of velocity and gradients of all flow variables in the direction normal to the boundary were set to zero. For the ground and the surfaces of the block, standard wall functions (Rodi, 1980) were used to calculate the source terms for K and ϵ . On the upwind boundary (inlet), K , ϵ , and the normal component of velocity were specified. The velocity was calculated according to a power-law profile, i.e. $U(z)/U_r = (z/z_r)^n$, where $U(z)$ is the velocity in the direction normal to the upwind boundary, U_r is a reference velocity at a reference height of z_r , and n is equal to 0.25; tangential components of the velocity were zero. Profiles for K and ϵ at the upwind boundary were derived from the velocity profile (Patterson and Apelt, 1989) and were comparable to turbulence intensities on the order of a few percent. At the downwind boundary (exit), normal gradients of all flow variables except pressure were set to zero.

The numerical solution was considered to have converged when the normalized residuals for the U , V , and W velocity components, pressure, K , and ϵ achieved a value of 10^{-3} or lower. In the case of 45° wind incidence, it was not possible to reduce the normalized residuals for K and ϵ below 5×10^{-3} , probably due to the assumption of steady flow (time-invariant). This assumption does not allow for adequate representation of temporal phenomena such as vortex shedding that may be inherent to the flow configuration (Castro and Robins, 1977).

2.2. Trajectories of rain drops

Trajectories of individual rain drops were calculated numerically according to

$$M \frac{dU_i^p}{dt} = F_{Di} - M\delta_{i3}g,$$

where $F_{Di} = (C_D \pi D_p^2 \rho / 4)(U_i - U_i^p)|U_i - U_i^p|$, M is the rain drop mass, U_i the air velocity in x_i direction, U_i^p the drop velocity in x_i direction, t the time, F_{Di} the drag force in x_i direction, g the gravitational constant, δ_{ij} the delta function; ($\delta_{ij} = 1$ if $i = j$, $\delta_{ij} = 0$ if $i \neq j$), C_D the coefficient of drag ($= f(\text{Re})$), D_p the drop diameter, ρ the density of air, ν the kinematic viscosity of air, and Re the sphere Reynolds number ($= D_p \sqrt{\sum_1^3 (U_i - U_i^p)^2} / \nu$).

C_D was obtained from empirical formulas for drag on a sphere (Morsi and Alexander, 1972). Trajectory calculations were performed for eight wind conditions, namely four values of wind speed ($U_r = 1.25, 2.5, 5, \text{ and } 10 \text{ m s}^{-1}$ at $z_r = 30 \text{ m}$) and two wind incidence angles (0 and 45°). For each of these conditions, trajectories of rain drops with diameters of 1.25, 2.5, and 5 mm were simulated. Rain drop evaporation, coalescence, or breakup were not considered, i.e. individual rain drop diameters were held constant at their initial values. In a limited number of cases, trajectories of 0.625 and 7.07 mm drops were also simulated. Results for those drop sizes, not presented here, were used for checking model consistency.

Approximately 4000 trajectories were calculated for each flow condition and drop diameter. Drops were released at a fixed height of 240 m. Initial positions were varied over a horizontal area. This area was large enough to include all release positions that could result in impaction on the surface of the block. The initial vertical velocity was set at the terminal velocity while the initial horizontal velocity was set at the air velocity, $U(z = 240 \text{ m})$. In selected cases, the effect of turbulence on fluxes of rain to surfaces of the block was evaluated using a Random Walk model (e.g. Thomson, 1987; Dai, 1999). While not negligible for trajectories of individual drops, the effect of turbulence was small when fluxes of rain to large sections of the block were considered as in the present study. Air flow fields around buildings and resulting trajectories of raindrops are

discussed at greater length by Choi (1993) and Karagiozis et al. (1997).

2.3. Meteorological data

A cup anemometer (Model 014A, Met One Instruments), wind vane (Model 024A, Met One Instruments), and tipping bucket rain gauge (Model 370, Micromet) were used to obtain meteorological data on the roof of Warner Hall on the Carnegie Mellon University campus over the period 4/29/98–6/18/98. Warner Hall is approximately one kilometer NE of the Cathedral of Learning. A datalogger (Model CR21X, Campbell Scientific) recorded the average wind speed, eight-bin frequency count for wind direction (45° per bin), and total rainfall amount for 15 min measurement intervals. The maximum instantaneous wind speed during each interval and the corresponding wind direction were also recorded. These data, intended to represent meteorological conditions upwind of the Cathedral of Learning, provided input parameters for calculations of rain fluxes to the block surfaces. The seven-week period included 21 d of rain. The overall rainfall during this period was equivalent to 1440 mm yr^{-1} . Sixteen percent of the rainfall over the period was contributed by two powerful thunderstorms on 6/2/98. The overall rainfall without those two thunderstorms was equivalent to 1210 mm yr^{-1} . The long-term rainfall rate for Pittsburgh is approximately 1000 mm yr^{-1} , with the months of May and June each contributing 10% of the annual rainfall. The 21 d of

rainfall contained 207 15 min interval of rain with an average rainfall intensity of 3.3 mm h^{-1} each (standard deviation = 5.7 mm h^{-1}).

While wind conditions and rain intensity are represented by continuous distributions, model calculations of individual rain drop trajectories were performed at discrete conditions, e.g. wind speed = 5 m s^{-1} , wind incidence angle = 0° , and rain drop diameter = 1.25 mm . Thus, for compatibility between trajectory calculations and the measured parameters, it was necessary to place meteorological data in discrete categories. Measured values of wind speed were placed in one of four bins, equal in size (in logarithmic space) and centered at 1.25, 2.5, 5, and 10 m s^{-1} . Similarly, measured wind directions were placed in one of eight categories, each spanning 45° . The categories were chosen so that the wind would always approach the model block at angles of 0 or 45° .

For each 15 min interval, the measured rain intensity was used to derive a discrete rain drop size distribution. The distribution consisted of only three drop sizes, having diameters of 1.25, 2.5, and 5 mm (Fig. 2); these rain drop sizes allowed for comparison of results with the earlier work of Choi (1993) who used comparable values. The calculation was based on the exponential distribution proposed by Marshall and Palmer (1948):

$$n(D_p) = n_0 \exp(-XD_p),$$

where $n(D_p) dD_p$ is the number of drops per cm^3 with diameter between D_p and $D_p + dD_p$, $n_0 = 0.08 \text{ cm}^{-4}$,

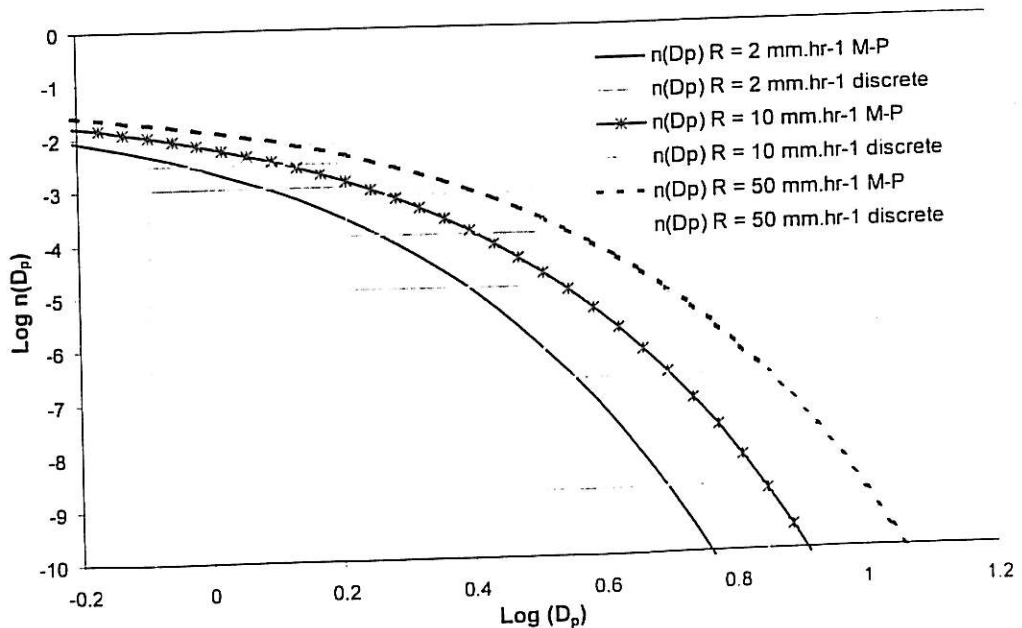


Fig. 2. Discrete size distribution and theoretical Marshall–Palmer Distribution for $R = 2, 10,$ and 50 mm h^{-1} . D_p is in mm; $n(D_p)$ is in cm^{-4} .

$X = 41R^{-0.21} \text{ cm}^{-1}$, D_p is the rain drop diameter (cm) and R is the rain intensity (mm h^{-1}).

Number concentrations for drops in the three size bins were multiplied by a correction factor so that the rain intensity due to drops with $D_p = 1.25, 2.5,$ and 5 mm was equal to the rain intensity measured at Warner Hall. Note that the instantaneous shape of the drop size distribution is expected to vary considerably. However, at long averaging times, the number concentration as a function of drop diameter may be adequately represented by an exponential distribution (Gori et al., 1988).

2.4. Rain impingement calculation

Each face of the block was divided into three vertical strips and five horizontal strips resulting in 15 rectangular sections of equal size, $10 \text{ m} \times 32 \text{ m}$ (Fig. 1). This facilitated comparison of modeling results with soiling patterns at the Cathedral as well as comparison of results with the earlier work of Choi (1993). In order to assess the effects of individual parameters on the delivery of raindrops to each of the 15 sections of the block, we adopted the Local Effect Factor (LEF) suggested by Choi (1993). For a given wind speed, incident flow orientation, and raindrop diameter (D_p), the LEF for a vertical section of the block is equal to the ratio (expressed as a percentage) of the flux m^{-2} of rain drops of diameter D_p to that section divided by the flux m^{-2} of rain drops of diameter D_p to the ground far away from any flow obstructions.

Total fluxes of rain to the vertical walls of the Cathedral of Learning were estimated by combining meteorological data collected at Warner Hall with LEFs calculated for a discreet set of flow conditions and raindrop sizes. The amount of rain delivered to each section of the model block was calculated for every 15 min interval (total of 207 intervals) that was associated with rainfall.

3. Results and discussion

3.1. Raindrop delivery to the block: effect of raindrop diameter and wind conditions

LEFs are shown for four wind speeds and three rain drop diameters in Fig. 3 for air flow perpendicular to the block (wind incidence angle = 0°). In general, LEFs increase with increasing wind speed and raindrop diameter for any given section of the block face. This result is intuitive since inertial impaction of raindrops onto the building face is expected to increase at higher wind speeds and raindrop sizes. The spatial variation of LEFs across the block face is more complex.

LEFs increase with height along the block. This is to be expected since near the top of the block, raindrops still retain much of their initial vertical and horizontal

momentum. At lower elevations, raindrops are moving slower in the stream-wise direction due to both the shape of the incident wind profile (power law) and the disturbance in the air flow caused by the presence of the block. Thus, it is less likely that a raindrop will impact on the lower sections of the block than on the higher sections. Variations of LEFs across the rows of the block are interesting, especially for the case where the wind speed is 10 m s^{-1} (Fig. 3d). For example, for $D_p = 1.25 \text{ mm}$, LEFs are lower at the center sections of the block (C1–C5) than they are at the outer sections (LS1–5 and RS1–5) in any given row. In contrast, for $D_p = 2.5 \text{ mm}$ the center sections of the block have higher LEFs than the outer sections except at the top row where they are comparable. The same is true for $D_p = 5 \text{ mm}$ except for the fourth row (LS4, C4, and RS4) where the center section is impacted by fewer raindrops than the side sections. These results are not an artifact of the resolution of the numerical model; changing the grid resolution for the CFD simulation or decreasing the time step in the Lagrangian trajectory calculations yields the same general behavior. More likely, these observations are due to the complex interaction of several phenomena including initial raindrop velocity, raindrop inertia, and the path that a raindrop follows. For example, raindrops with large diameters have higher terminal velocities than smaller drops. Consequently, the trajectories of large drops more closely approximate a vertical line than those of smaller drops. In order to impact the block, large drops have to follow a path that is closer to the block face than smaller drops. Therefore, these larger drops are more likely to interact with airflow immediately adjacent to the block, which is in an upward direction.

The results obtained in the present study for the block representing the Cathedral of Learning with relative dimensions of (1 : 1 : 5.3) compare favorably with those that were reported by Choi (1993) in Fig. 4 for a building with relative dimensions of (1 : 1 : 4). Choi reported similar trends for changes in LEFs with changes in wind speed, raindrop size, and elevation along the building face. We note however, that values reported by Choi for raindrops with $D_p = 1, 2,$ and 5 mm are generally higher than those presented here for $D_p = 1.25, 2.5,$ and 5 mm . This discrepancy is especially noticeable for the cases where the wind speed is 5 m s^{-1} (Figs. 3c and 4a). The two studies employ slightly different formulations of the CFD and Lagrangian trajectory models. In addition, we attribute much of the differences between the two sets of results to the different wind speeds and possibly different building heights (not reported by Choi).

Fig. 5 shows LEFs for air flowing past the block at an oblique angle of 45° . Note that in this case, there are two windward faces that are expected to behave identically owing to the symmetry of the flow. Air is flowing from left to right in this figure, i.e. the left side of the block corresponds to the leading edge on the windward face. In

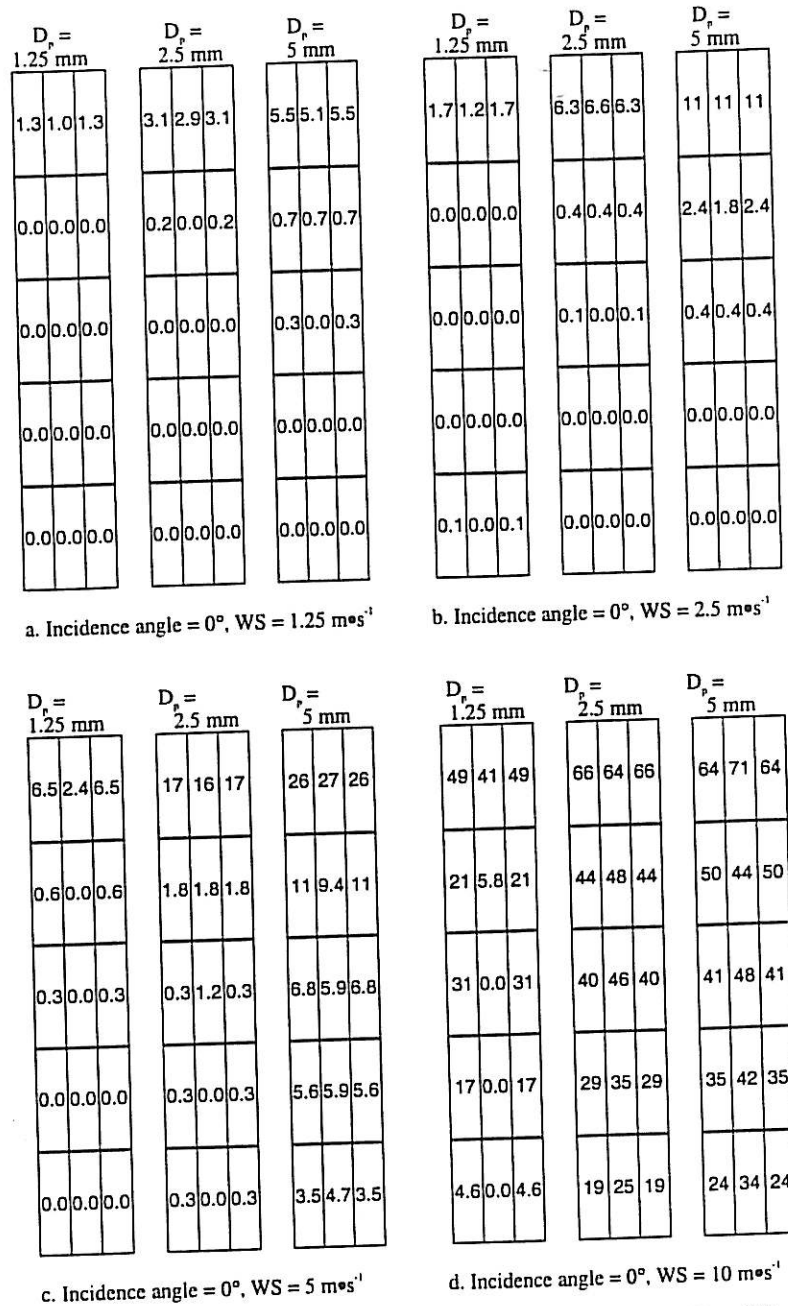


Fig. 3. Local Effect Factors (expressed as percentages) for rectangular block with dimensions of 30 m × 30 m × 160 m when the wind is perpendicular to block face (0° incidence angle) for raindrops with $D_p = 1.25, 2.5, \text{ and } 5 \text{ mm}$. (a) wind speed = 1.25 m s⁻¹, (b) wind speed = 2.5 m s⁻¹, (c) wind speed = 5 m s⁻¹, (d) wind speed = 10 m s⁻¹.

general, for any given row, LEF values are highest at the upstream section (LS), lowest at the downstream section (RS), and intermediate at the center section (C). It is interesting that for wind speeds of 1.25, 2.5, and 5 m s⁻¹, drops with $D_p = 1.25 \text{ mm}$ have higher LEFs at sections LS1–4 compared to drops with $D_p = 2.5$ and 5 mm. At

wind speeds of 10 m s⁻¹ the highest LEFs for those sections are for $D_p = 2.5 \text{ mm}$, followed by $D_p = 5 \text{ mm}$. As in the case of flow normal to the block face, we attribute these counterintuitive results to the differences in terminal velocities of the raindrops. Smaller drops fall more slowly and therefore the angle of their trajectory

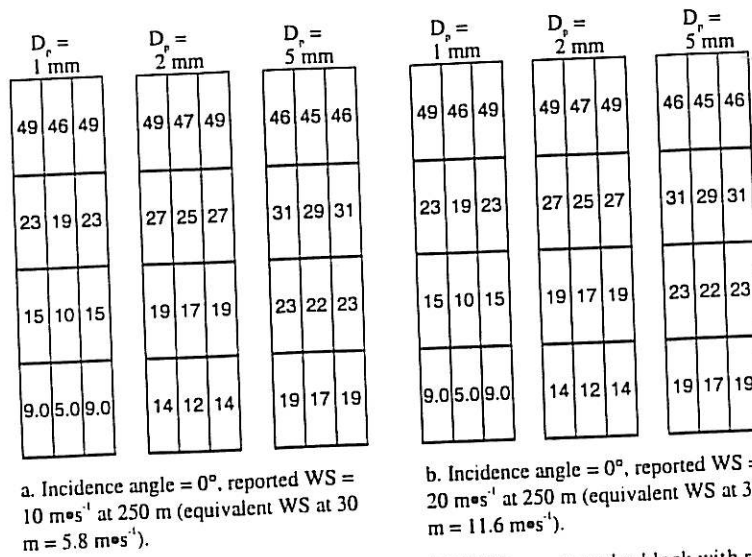


Fig. 4. Local Effect Factors (expressed as percentages) reported by Choi (1993) for rectangular block with relative dimensions of 1 : 1 : 4 for wind blowing perpendicular to block face (0° incidence angle) for raindrops with D_r = 1, 2, and 5 mm. (a) wind speed = 10 m s⁻¹ at 250 m (equivalent to 5.8 m s⁻¹ at 30 m for comparison with Fig. 3), and (b) wind speed = 20 m s⁻¹ (equivalent to 11.6 m s⁻¹ at 30 m for comparison with Fig. 3).

with respect to the block face is sharper than larger drops whose trajectories are closer to being parallel to the block. Note that this effect is enhanced in the case of air flowing at 45°. As the wind speed is increased, inertial effects become more important and larger drops are more likely to impact on the block than follow the flow around the block. This contributes to the result that LEFs are higher for 2.5 mm drops than for 1.25 mm drops at 10 m s⁻¹.

3.2. Raindrop delivery to the block: results using April–June 1998 meteorological data

Fig. 6 shows the fraction of time, the magnitude of the wind speed, and the average rain intensity associated with each wind direction during the rain events in the period 29 April–18 June, 1998. Note that the most common wind directions during rain events were W and SE, although both wind speed and rain intensity were greater during W winds. Fig. 7 shows modeling results for rain-water fluxes to surfaces of the block using the meteorological data that are summarized in Fig. 6. Sketches of the patterns of soiling at the Cathedral of Learning also appear in the figure. The faces of the block and the corresponding sides of the Cathedral of Learning have been labeled with names of nearby streets. The meteorological data have been used with calculated LEFs to estimate the annual flux of rain to each section of the block. On 6/2/98 two unusually severe thunderstorms with very high winds (gusts > 25 m s⁻¹) and intense

rainfall swept through the Pittsburgh area. In Fig. 7 numbers shown in black correspond to fluxes of rain excluding the 6/2/98 storms. The inclusion of the thunderstorms has profound effects on the magnitude of estimated rain fluxes, especially for the Fifth Avenue and Bellefield Avenue faces. A storm of such intensity, possibly related to El Niño, is a rare occurrence in Pittsburgh and its inclusion in the seven-week data set is likely to lead to biased estimates of rain fluxes to the Cathedral of Learning for other time periods; thus, the following discussion focuses on rain fluxes calculated without these storms. However, in Figs. 7–10, rain fluxes calculated with these two storms are displayed in gray italics for completeness of data presentation.

There is reasonable, although not exact, correspondence between areas on the façade of the Cathedral of Learning that are white and sections of the block that receive the most rain. The Bigelow Boulevard and Fifth Avenue faces have high values of rain flux whereas the Forbes Avenue and Bellefield Avenue faces have lower values. This result qualitatively supports the hypothesis that soiling patterns at the Cathedral of Learning are determined to a large extent by delivery of rain to the building surfaces.

Despite differences in magnitude, patterns of rain delivery are similar for all four faces. For example, the amount of rain delivered to each face is highest at the top row (LS5, C5, and RS5) and is higher at the side sections (LS and RS) than the center sections (C). However, while fluxes to the left (LS) and right (RS) sections of the Forbes

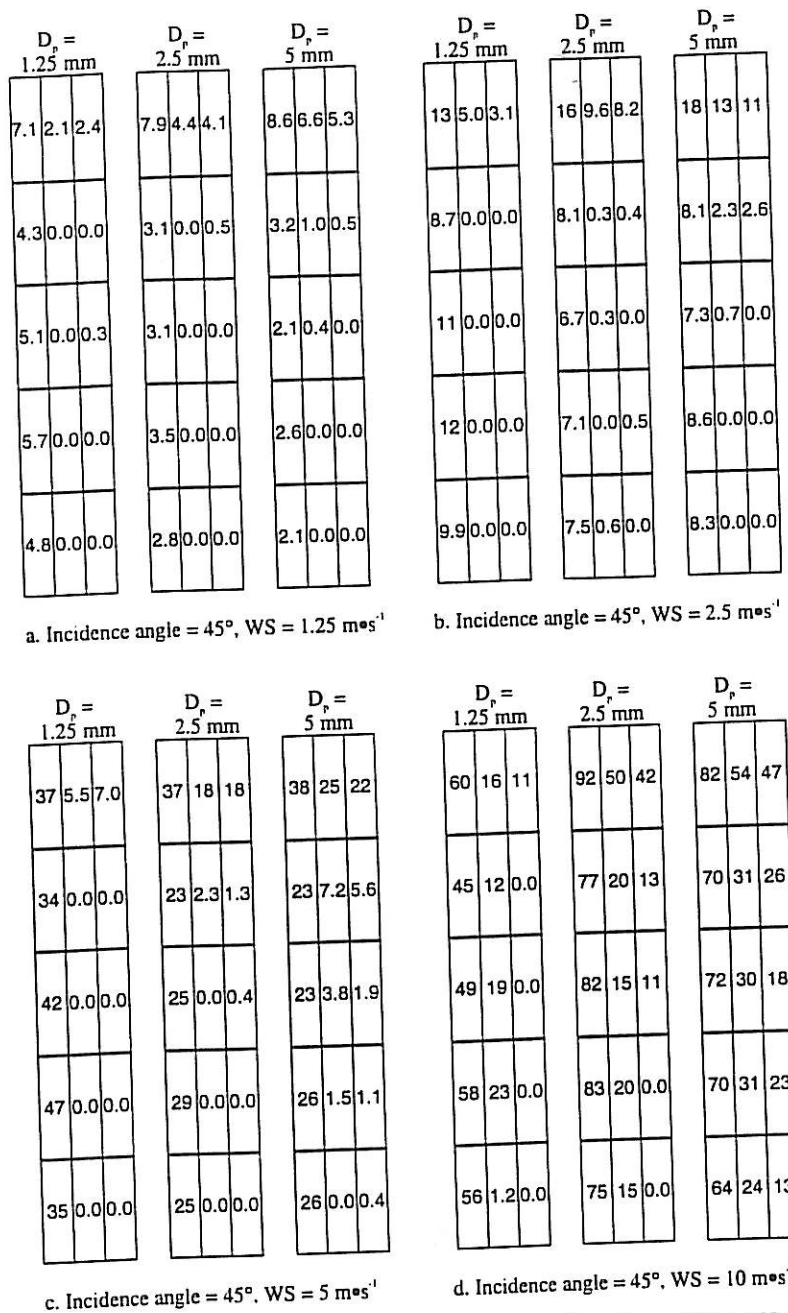


Fig. 5. Local Effect Factors (expressed as percentages) for rectangular block with dimensions of 30 m × 30 m × 160 m when the wind is oblique to block face (45° incidence angle) for raindrops with D_p = 1.25, 2.5, and 5 mm. The left edge of the block face represents the leading edge. (a) wind speed = 1.25 m s⁻¹, (b) wind speed = 2.5 m s⁻¹, (c) wind speed = 5 m s⁻¹, (d) wind speed = 10 m s⁻¹.

Avenue face are approximately equal, they are significantly higher on the left sides of the Bigelow Boulevard face than on the right side. The opposite is true for the Fifth and Bellefield Avenue faces.

Some of these observations are explained by the meteorology during the measurement period. Impingement

of rain on the block surfaces is expected to be the greatest when the wind direction is favorable, wind speeds are high, and rainfall is intense. The high speeds of N, NW, W and SW winds combined with high rain intensities contribute to increased fluxes to the Fifth Avenue and Bigelow Boulevard faces as compared with Forbes and

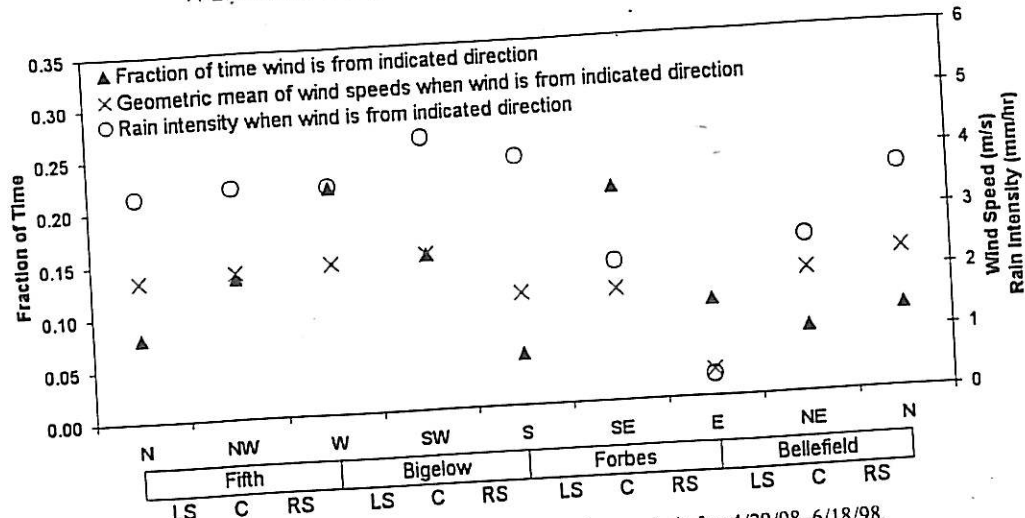


Fig. 6. Meteorological conditions during rainy periods for 4/29/98-6/18/98.

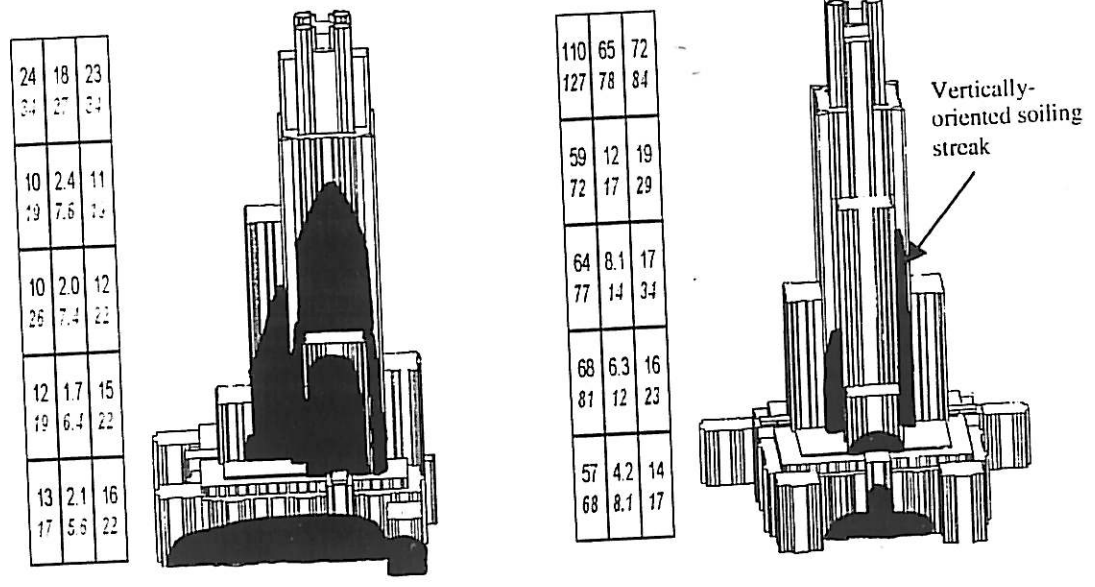
Bellefield Avenues. The low frequency of winds from the south result in lower fluxes to the right side of Bigelow Boulevard and the left side of Forbes Avenue. On the right side of Forbes Avenue and the left side of Bellefield Avenue, very low wind speeds and rain intensities also result in low fluxes of rain. This renders fluxes of rain to the Forbes Avenue face approximately symmetric with respect to the vertical centerline (C1-5), but higher rain intensities for N winds result in higher fluxes to the right side of the Bellefield Avenue face than the left side.

It is interesting that the right side of the Bigelow Boulevard face is white despite low values of rain fluxes. This may be the result of a large protrusion on the Bigelow Boulevard side that is not included in the block used in the model (Figs. 1 and 7b). The fluxes of rain to the protrusion are likely to be much higher than they would be to the large block in the absence of the protrusion. It is also interesting that the vertical streak of soiling on the left side of the Cathedral is smaller than that on the right side. This is qualitatively consistent with the asymmetry of the estimated rain fluxes to the Bigelow Boulevard face.

The right side sections (RS1-4) of the Bellefield Avenue face are soiled even though the fluxes of rain to those sections are much higher than the fluxes of rain to some of the white, center sections (C1-C4) on the Fifth Avenue face. This may be the result of using a limited meteorological data set and a greatly simplified geometry. In addition, the block used in the numerical model is smooth whereas the Cathedral is a complex structure that has roughness on several scales. For example, the Cathedral has vertically oriented decorative features that span a large fraction of the building height (Fig. 1). These structures can enhance the delivery of rain to sections of

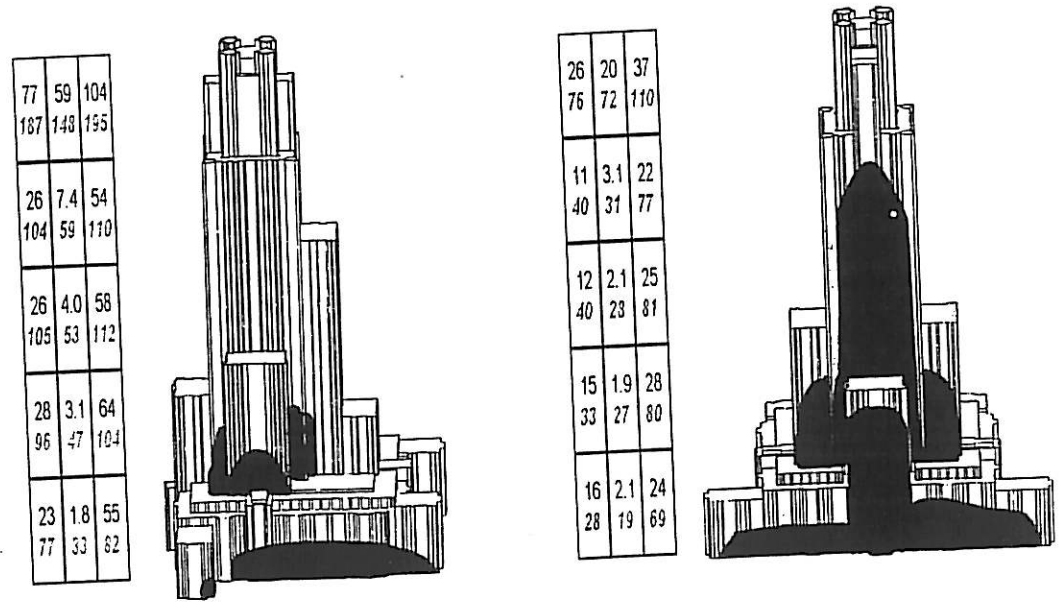
the Cathedral by capturing raindrops that would otherwise follow the air flow around the Cathedral. Furthermore, the model does not account for the runoff of water. Note that rain fluxes to the top rows (LS5, C5, and RS5) of the Fifth Avenue and the Bigelow Boulevard faces are quite high. If the stone at those sections becomes saturated, rainwater will run down the wall to lower sections, possibly eroding the stone as it falls. Thus, the extent of soiling on a particular section of the Cathedral depends not only on the rain fluxes to that particular section, but also on rain fluxes at higher elevations on the wall. However, we note that visual inspection of the limestone during light-to-moderate rainfall suggests that most of the water is absorbed into the stone close to the point of impact.

It is instructive to consider how different meteorological conditions contribute to the total fluxes of rain to sections of the Cathedral of Learning. In Fig. 8, the fluxes of rain are categorized by wind speed. For brevity, results are only presented for Forbes Avenue (heavily soiled) and Fifth Avenue (primarily white). For both the Forbes and Fifth Avenue sides, most of the rain is delivered to the block at wind speeds of 2.5 and 5 m s⁻¹. While the highest LEFs are associated with a wind speed of 10 m s⁻¹ (Fig. 3), the occurrence of such wind speeds is somewhat rare. On the other hand, at wind speeds of 1.25 m s⁻¹, the LEFs are quite small. Thus, moderate LEFs combined with high frequencies of occurrence cause the intermediate wind speeds to be the greatest contributors to rain fluxes. However, by including the two large storms on 6/2/98 in the data set (numbers in gray italics), it can be seen that even a few occurrences of high winds during rainfall can have an appreciable effect on the total fluxes of rain to sections of the block.



a. Forbes Avenue (Facing SE)

b. Bigelow Boulevard (Facing SW)



c. Fifth Avenue (Facing NW)

d. Bellefield Avenue (Facing NE)

Fig. 7. Rain fluxes (mm yr^{-1}) to sections of rectangular block during 4/29/98–6/18/98, shown with soiling patterns at the Cathedral of Learning. Numbers in gray italics are for a data set that includes two large thunderstorms on 6/2/98. The average rainfall intensity over the same period was 1210 mm yr^{-1} (1440 mm yr^{-1} including 6/2/98 storms).

Consequently, much of the rain delivery to a building surface may result during gusts of wind which can be significantly larger in magnitude than the average wind speed for a given interval. For example, the average wind

speeds for rainy 15 min measurement intervals have a geometric mean of 2.2 m s^{-1} (geometric standard deviation, $\sigma_g = 1.7$) while maximum wind speeds have a geometric mean of 3.9 m s^{-1} ($\sigma_g = 1.7$). The data obtained at

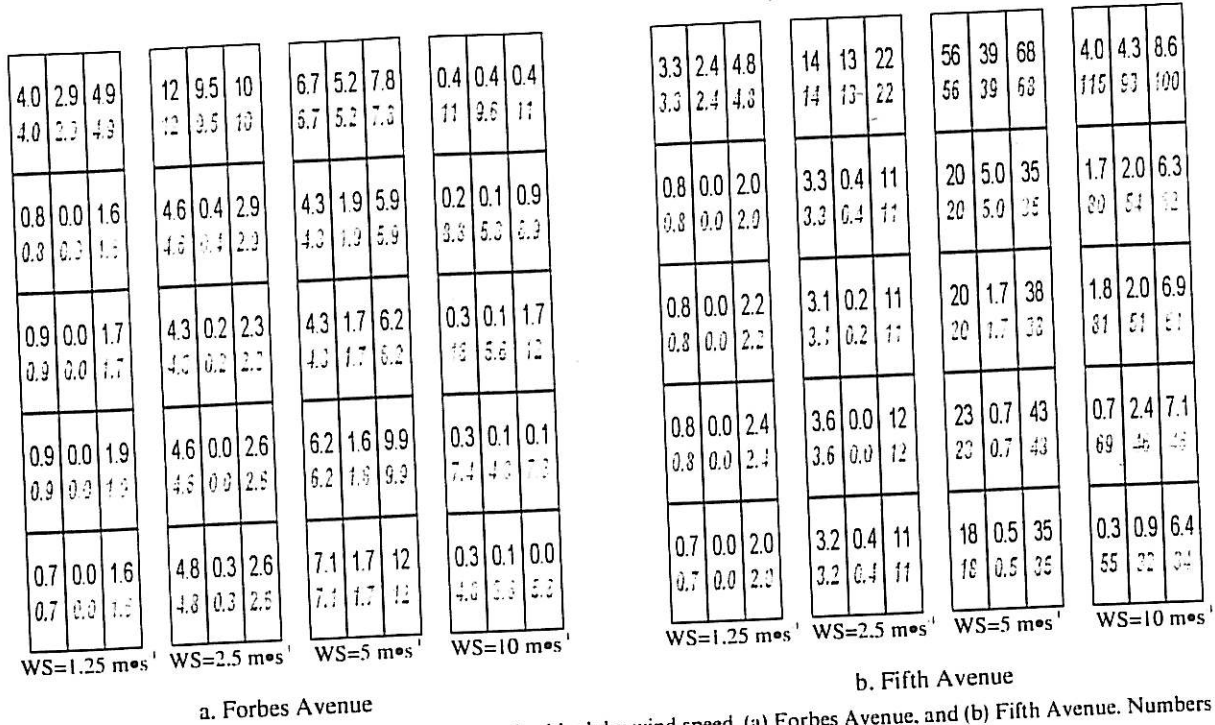


Fig. 8. Rain fluxes (mm yr^{-1}) to sections of the rectangular block by wind speed. (a) Forbes Avenue, and (b) Fifth Avenue. Numbers in gray italics are for data set that includes two large thunderstorms on 6/2/98.

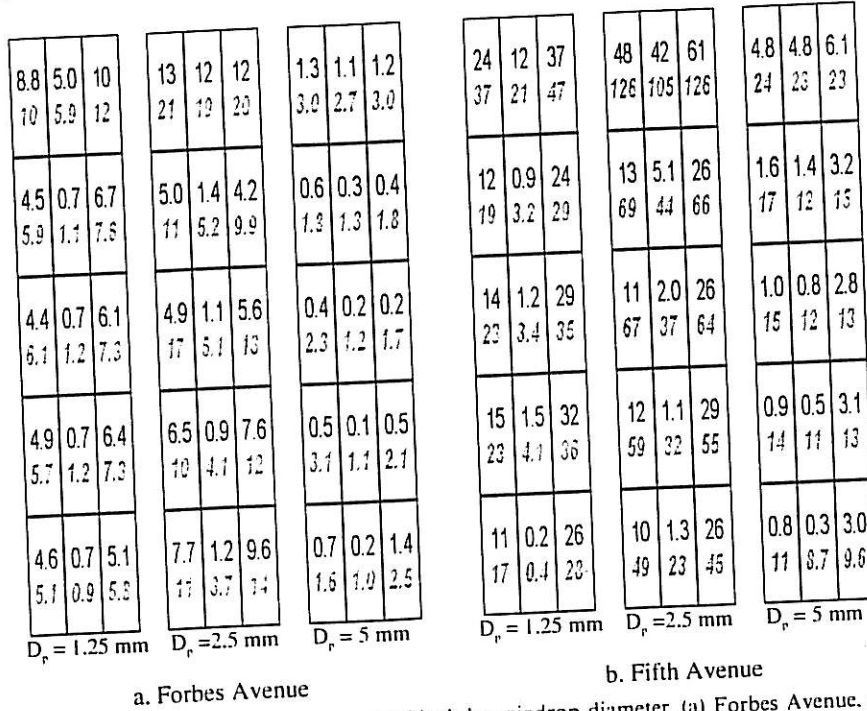


Fig. 9. Rain fluxes (mm yr^{-1}) to sections of the rectangular block by raindrop diameter. (a) Forbes Avenue, and (b) Fifth Avenue. Numbers in gray italics are for data set that includes two large thunderstorms on 6/2/98.

Warner Hall also show a positive correlation between wind speed and rain intensity ($\rho = 0.31$), further illustrating the importance of accurately accounting for rain events associated with high winds.

In Fig. 9, the contributions to rain fluxes are categorized by raindrop diameter. According to the raindrop size distribution used in the present model (Fig. 2), the rainfall amounts associated with 1.25, 2.5, and 5 mm

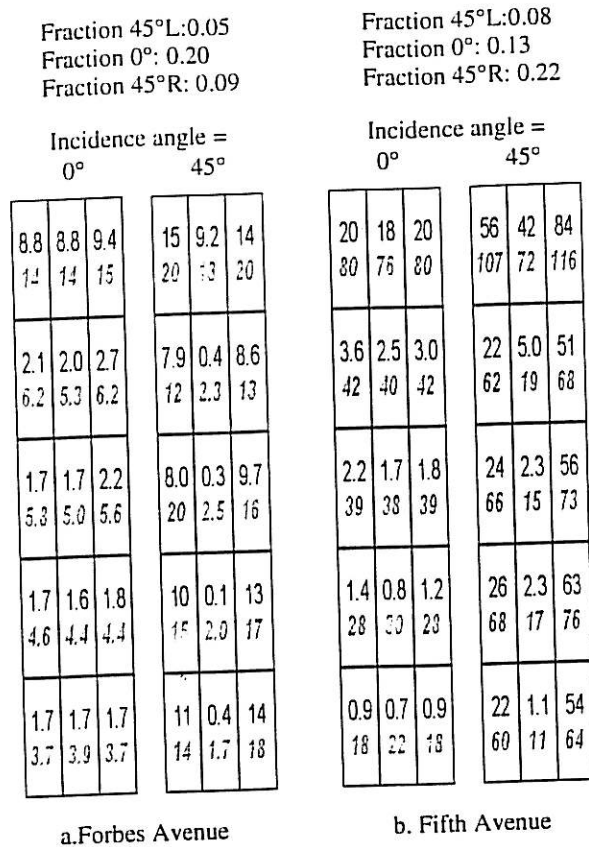


Fig. 10. Rain fluxes (mm yr^{-1}) to sections of the rectangular block by wind direction. (a) Forbes Avenue, and (b) Fifth Avenue. Figure also shows the fraction of time wind-is-blowing perpendicular to the face and at an oblique angle from the left and the right. Numbers in gray italics are for data set that includes two large thunderstorms on 6/2/98.

drops are 578, 557, and 74 mm yr^{-1} , respectively. LEFs are generally higher for 5 mm drops than for 1.25 and 2.5 mm drops, but the low abundance of 5 mm drops results in their relatively small contribution to total rain fluxes. Compared to the other sizes, drops with a diameter of 1.25 mm deliver the least rain to the center sections of the faces while drops with a diameter of 5 mm contribute the least to the outer sections.

The effect of wind incidence angle on rain flux is illustrated in Fig. 10. Note that the wind can be incident to a face at 45° from either the left or right side of that face. Significant amounts of rain are delivered to both the Forbes and the Fifth Avenue faces when the wind angle is 45° . The importance of considering oblique wind angles is illustrated by the data for Forbes Avenue, where more of the rain is associated with a wind angle of 45° than 0° , even though the former wind incidence angle occurs less frequently than the latter.

In addition to better approximating the geometry of a building, future modeling efforts should consider

the temporal variations in the flow field. Here, the flow field was assumed to be at steady state with respect to the Reynolds averaged Navier–Stokes, K , and ϵ equations, although this is likely to be far from actuality for a building in an outdoor environment. Furthermore, even when upstream flow conditions are invariant with time, there may be time-dependent phenomena on the building scale. Such phenomena, occurring primarily at oblique wind incidence angles, include sudden shifts in the location of the stagnation point on the windward side of the building and vortex shedding on the leeward side of the building (Castro and Robins, 1977; Hosker, 1984). This effect is not accounted for in the present model.

4. Conclusions

A numerical model was used to investigate rain impingement on a tall limestone building and the influence of rain on soiling patterns. The RNG K – ϵ model was used to compute the steady-state air flow field around a $30 \text{ m} \times 30 \text{ m} \times 160 \text{ m}$ rectangular block, representing the Cathedral of Learning in Pittsburgh, Pennsylvania for several wind conditions. These included four wind speeds – 1.25, 2.5, 5, and 10 m s^{-1} – and two wind incidence angles – 0 and 45° . Next, trajectories of individual rain drops in the computed flow field were calculated and the fraction of those drops impinging on the block surface was determined. This was done for each wind condition and for each of three drop diameters, 1.25, 2.5, and 5 mm. Though there were differences, calculated Local Effect Factors compared favorably with the earlier work of Choi (1993).

Meteorological data were measured in 15 min intervals near the Cathedral of Learning over a period of seven weeks. For modeling purposes, measured wind speeds were placed in one of four categories that coincided with the wind speeds used to calculate the flow field around the block. A discrete distribution containing eight categories, each representing a wind incidence angle of 0 or 45° to a face of the block, was used for measured values of wind direction. Similarly, a discrete rain drop size distribution containing only 1.25, 2.5, and 5 mm drops was based on measured rain intensities and the Marshall–Palmer size distribution (Marshall and Palmer, 1948). These modified meteorological data were used to calculate the flux of rain to the four faces of the model block.

The calculated rain fluxes to the faces of the block were reasonably consistent with observed soiling patterns at the Cathedral. White areas on the Cathedral walls generally corresponded to sections receiving high fluxes of rain. Conversely, soiled areas on the Cathedral generally corresponded to sections receiving less rain. Most of the

rain flux was attributable to intermediate wind speeds of 2.5 and 5 m s⁻¹. However, results indicated that high wind speeds can have a significant contribution under some conditions, especially since rain intensities and wind speeds tend to be positively correlated. More rain was delivered to the block in the form of 2.5 mm drops than either 1.25 or 5 mm drops. A large fraction of delivery of rain was a result of wind incident at 45° to the block, underscoring the importance of considering oblique wind approach angles for delivery of rain to buildings. While a block was used to represent the Cathedral of Learning, discrepancies between estimated rain fluxes and soiling patterns indicated that additional detail in the geometry of the physical model is needed to better estimate delivery of rain to building surfaces.

Acknowledgements

This work was funded by the National Park Service Cooperative Agreements 042419005 and 00196035. Thanks to Curt Yeske and Shawn McClory who provided invaluable technical support. We appreciate the help from Paul Sides, Rob Verrenna, and the Department of Chemical Engineering on software issues. Christina Amon provided insightful suggestions for the preparation of this manuscript. Thanks are also due to Rich Palladini and Larry Young for permitting access to Warner Hall. Ivan Locke, David Iorio, and Judy Lee contributed to the CAD model of the Cathedral of Learning shown in Fig. 7. Thanks to John Murray and Ivan Locke for their measurement work at the Cathedral of Learning. A special thanks to Susan Sherwood for her invaluable insights and guidance during the early phases of this work.

References

- Amoroso, G.G., Fassina, V., 1983. Stone Decay and Conservation: Atmospheric Pollution, Cleaning, Consolidation and Protection. Materials Science Monographs 11. Elsevier, Amsterdam.
- Castro, I.P., Robins, A.G., 1977. The flow around a surface-mounted cube in uniform and turbulent streams. *Journal of Fluid Mechanics* 79, 307–335.
- Choi, E.C.C., 1993. Simulation of wind-driven rain around a building. *Journal of Wind Engineering and Industrial Aerodynamics* 46, 721–729.
- Dai, W., 1999. Numerical and Wind Tunnel Studies of Particle Transport, Deposition, and Rebound in Turbulent Flows. Ph.D. Dissertation, Carnegie Mellon University, Pittsburgh, Pennsylvania, April 1999.
- Davidson, C.I., Tang, W., Finger, S., Etyemezian, V., Striegel, M.F., Sherwood, S.I., 1999. Soiling patterns on a tall limestone building: Changes over 60 years. *Environmental Science and Technology*. In press.
- Etyemezian, V., Davidson, C.I., Finger, S., Striegel, M., Barabas, N., Chow, J., 1998. Vertical gradients of pollutant concentrations and deposition fluxes at a tall limestone building. *Journal of American Institute for Conservation* 37 (2), 187–210.
- Giles, M.J., 1994. Turbulence renormalization group calculations using statistical mechanics methods. *Physics of Fluids* 6, 595–604.
- Gori, E., Rafanelli, C., Aslan, Z., 1988. Variations in rain drop size distributions measured at Rome. *Nuovo Cimento C* 11 (5–6), 679–692.
- Hosker, Jr., R.P., 1984. Flow and diffusion near obstacles. In: Randerson, D. (Ed.), *Atmospheric Science and Power Production Report for United States Department of Energy*.
- Karagiozis, A., Hadjisophocleus, G., Cao, S., 1997. Wind-driven rain distributions on two buildings. *Journal of Wind Engineering and Industrial Aerodynamics* 67 & 68, 559–572.
- Lauder, B.E., Spalding, D.B., 1974. The numerical calculation of turbulent flows. *Computer Methods in Applied Mechanics and Engineering* 3, 269–289.
- Livingston, R.A., 1992. Graphical methods for examining the effects of acid rain and sulfur dioxide on carbonate stones. In: Delgado Rodrigues, J., Henriques, F., Telmo Jeremias, F. (Eds.), *Proceedings of the seventh International Congress on Deterioration and Conservation of Stone*. Lisbon, Portugal.
- Marshall, J.S., Palmer, W.McK., 1948. Relation of raindrop size to intensity. *Journal of Meteorology* 5, 165–166.
- Minson, A.J., Wood, C.J., Belcher, R.E., 1995. Experimental velocity measurements for CFD validation. *Journal of Wind Engineering and Industrial Aerodynamics* 58, 205–215.
- Morsi, S.A., Alexander, A.J., 1972. An investigation of particle trajectories in two-phase flow systems. *Journal of Fluid Mechanics* 55, 193–208.
- Murakami, S., Mochida, A., Ooka, R., Kato, S., Iizuka, S., 1996. Numerical prediction of flow around a building with various turbulence models: comparison of *k-ε* EVM, ASM, DSM, and LES with wind tunnel tests. *ASHRAE Transactions* 102, 741–753.
- Ogawa, Y., Oikawa, S., Uehara, K., 1983. Field and wind tunnel study of the flow and diffusion around a model cube-I. Flow measurements. *Atmospheric Environment* 17, 1145–1159.
- Patterson, D.A., Apelt, C.J., 1989. Simulation of wind flow around three-dimensional buildings. *Building and Environment* 24, 39–50.
- Rodi, W., 1980. Turbulence Models and their Application in Hydraulics. International Association for Hydraulics Research (IAHR), Delft, the Netherlands.
- Selvam, R.P., 1996. Numerical simulation of flow and pressure around a building. *ASHRAE Transactions* 102, 765–772.
- Sherwood, S.I., Gatz, D.A., Hosker Jr., R.P. et al., 1990. Processes of deposition to structures. NAPAP SOS/T Report 20. In: National Acid Precipitation Assessment Program. Acidic Deposition: State of Science and Technology, Vol. III. September.
- Sulem, P.L., Fournier, J.D., Pouquet, A., 1979. Fully developed turbulence and renormalization group. *Proceedings of the*

- International Conference on Dynamical Critical Phenomena and Related Topics, Switzerland, 2–6 April.
- Tang, W., Davidson, C.I., Finger, S., 1999. Environmental exposure effects on an historic stone building. Report to the United States National Park Service, October 1999.
- Thomson, D.J., 1987. Criteria for the selection of stochastic models of particle trajectories in turbulent flows. *Journal of Fluid Mechanics* 180, 529–556.
- Zhou, Y., Stathopoulos, T., 1996. Application of two-layer methods for the evaluation of wind effects on a cubic building. *ASHRAE Transactions* 102, 754–764.